Industrial Demand Side Management of a Steel Plant Considering Alternative Power Modes and Electrode Replacement

Pedro M. Castro,[a,1] Giancarlo Dalle Ave[b,c] ,Sebastian Engell[c],

Ignacio E. Grossmann[d] and Iiro Harjunkoski[b]

[a] Centro de Matemática Aplicações Fundamentais e Investigação Operacional, Faculdade de Ciências, Universidade de Lisboa, 1749-016 Lisboa, Portugal

[b] ABB Power Grids Research, Kallstadter Str. 1, 68309 Mannheim, Germany

[c] Process Dynamics and Operations Group, Department of Biochemical and Chemical Engineering, Technische Universität Dortmund, Emil-Figge-Str. 70, 44221 Dortmund, Germany

[d] Center for Advanced Process Decision-Making, Department of Chemical Engineering, Carnegie Mellon University, Pittsburgh, PA 15213, USA

Abstract

As a major energy consumer, steel plants can help to stabilize the power grid by shifting production from periods with high demand. Electric arc furnaces can be operated at different power levels, affecting energy efficiency, duration of melting tasks and the rate of electrode degradation, which has previously been neglected. We thus propose a new mixed-integer linear programming (MILP) formulation for the optimal scheduling under time-of-use electricity pricing that captures the tradeoffs involved. It relies on the Resource-Task Network (RTN) for modeling processing tasks with variable

---

[1] Corresponding author. E-mail: pmcastro@fc.ul.pt.

electrode mass depletion and replacement tasks that regenerate the mass. Through the results of an industrial case study, we show that the high-power mode is mostly avoided, despite allowing for more processing tasks in low-price periods. This is because such mode is less energy efficient and consumes a larger mass of electrode, indicating that electrode replacement plays an important role in total cost minimization.

1. Introduction

As electricity generation becomes more and more focused on renewables such as wind and solar, new methods are needed to ensure that the electricity grid remains balanced at all times. One such method to contribute to this stability is Demand Side Management (DSM). DSM refers to different methods of shaping the energy demand curve at the consumers' side. On the one hand, this benefits electricity suppliers through flattened load curves, enabling a quicker reaction to mismatch in the grid. On the other hand, DSM provides a method for consumers to lower their operating costs by adapting the production to time-dependent electricity prices.

Due to the strong time-dependence of these energy-related concerns, effective scheduling is essential in DSM, and it has been identified as a key challenge in industrial deployment of scheduling solutions, especially when a complex manufacturing process is involved[1,2]. Therefore, many recent studies have looked at various aspects of DSM applied to a variety of industries including air separation[3-6], cement making[7-9], combined heat and power plants[10-11] and pulp-and-paper[12].

In general, the more energy intensive an industry is and the more flexibility the manufacturing process has, the more can be gained from participating in DSM schemes. As a result, the steelmaking industry has been identified as a key industry for DSM because EAFs, which are used to melt solid steel, consume large amounts of energy and offer considerable flexibility in when and how they are operated. The flexibility when operating the EAFs stems from the fact that they are operated in batch mode and can change their power consumption rates based on the setting of the on-load tap changer[13].

This enables effective response to time-varying prices, as the timing of batches and the batch energy-intensity can easily be changed.

Scheduling and DSM have been studied by a wide variety of authors. Nolde and Morari[14] proposed a continuous-time scheduling formulation for electricity load tracking of a steel plant. The problem they consider involves scheduling the production tasks, with fixed power consumption and duration, to track a predefined energy curve, with penalties for deviating from said curve. Hadera et al.[15] studied the same problem but used a more efficient formulation than their predecessors while simultaneously accounting for multiple electricity purchasing contracts. Pan et al.[16] proposed a mixed-integer nonlinear formulation (MINLP) for electrical load tracking under time-of-use (TOU) tariffs, where constraints are also derived for each of the six possible cases identified by Nolde and Morari[14]. Perhaps due to the increasing complexity from modeling TUO tariffs that change with load intervals, no attempt has been made to solve the resulting MINLPs by commercial solvers. Instead, the authors use an evolutionary algorithm that is shown capable of generating high-quality schedules. In the MINLP formulation of Xu et al.[17], the continuous casting stage is modeled more accurately, with the optimization deciding the casting time for each charge/heat as well as the casting speed. Nonlinear terms appear due to the product of continuous and binary variables, which are linearized exactly, while the bilinear and monomial terms involving the time and speed variables are relaxed using McCormick envelopes[18]. A three-stage MILP-NLP decomposition strategy coupled with spatial branch-and-bound is then used to obtain good-quality solutions in reasonable times.

Despite many authors relying on continuous-time formulations, the discrete-time representation is generally computationally more efficient when dealing with time-dependent utility pricing and availability[19,20]. Castro et al.[21] formulated the DSM problem for steel plants using a Resource-Task Network (RTN) formulation. The RTN[22] is a generic framework to model and optimize the scheduling of complex processes in a systematic way. Because of this, several other works have built upon the seminal RTN formulation for steel scheduling. Dalle Ave et al.[23] expanded the original

model by accounting for more detailed electricity market concerns, including the separation between intraday and day-ahead markets. Zhang et al.[13] added additional DSM flexibility by considering alternative operating modes for the EAFs. Operating modes have specific values for instantaneous electricity consumption as well as batch duration, and so electricity cost savings can come from both the timing of the batch, as well as the mode at which it is operated. However, each mode had the same total energy consumption, which is not accurate since energy efficiency for this system decreases as power consumption increases.

Another aspect of scheduling that has been gaining attention recently is the integration of equipment condition and maintenance into production planning/scheduling. Castro et al.[24] took seasonal electricity prices into account when optimizing the regular maintenance plan of a gas engine power plant supplying base load electricity to a chemical complex and selling excess production to the power grid. Maintenance of the gas engines was performed within a given time window of hours spent online. Zulfaki and Kopanos[25] addressed the simultaneous planning, maintenance and demand response of integrated production and utility systems, assuming that the power consumption for utility units increases linearly with the cumulative operation time and the degradation rate. Full performance could be recovered through offline cleaning, while online cleaning retrieved part of the condition (20% for a compressor network). The planning horizon was one month with electricity prices changing every day.

Nie et al.[26] considered a representative example of mixed batch/continuous processes in the chemical industry, where the processing capacity of a continuous unit is consumable and needs to be replenished offline after reaching a threshold limit of 25%. While the condition of the unit depends on the cumulative amount processed, it doesn't seem to affect the processing rate. Vieira et al.[27] studied the optimal planning of a continuous biopharmaceutical process considering decaying production yield.

Other applications can be found in the polymers industry[28], where each of the products contributes differently to the fouling of the polymerization reactor. The level of fouling cannot cross a specific threshold and contributes to an increase in batch time. From a fleet management perspective, Spüntrup et al.[29] looked at the maintenance scheduling of a compressor fleet. The authors assume that the compressors are always operating at full capacity, unless a maintenance activity is occurring, and consider two types of degradation indicators: fouling-type; and remaining useful lifetime (RUL). Another example comes from the work of van der Klauw et al.[30], who consider an energy storage system to reduce the electricity production peaks. They account for degradation based on the number of switches between charging and discharging cycles with a goal of maximizing the total energy throughput.

The integrated maintenance and production scheduling has also been studied in the context of steel plants. Biondi et al.[31] studied the simultaneous planning and scheduling of production and long-term maintenance in a steel plant, using the RUL of the ceramic lining of production units as the key degradation indicator. The goal of their optimization was to minimize operating costs including inventory and maintenance costs. The authors also presented an extension of the State-Task Network, adding constraints to account for the reduction of residual lifetime every time a task is performed, which can be restored by performing maintenance. It was modified by Wiebe et al.[32] to incorporate uncertain sensor data regarding equipment degradation using adjustable robust optimization. Failure probabilities were estimated with either a frequency or Markov Chain approach, while Bayesian optimization was used to efficiently optimize the box uncertainty set. It allowed obtaining lower cost solutions than random search and achieving a good compromise between preventive and corrective maintenance.

In this work, we also optimize the integrated production and maintenance of steel plants but on a shorter timescale, within the DSM setting, which has never been done before. The degradation considered is that of the furnace's electrode system, which occurs much faster than the lining of the

units, is greatly influenced by the operating power of the furnace and the production sequence[33]. The main merit of the paper is to integrate in one cost function, hourly-changing electricity prices, electrode degradation and production throughput, so as to find rigorous optimal production strategies. This is important because the cost of maintaining the electrodes, previously ignored, is almost as high as the electricity cost.

The rest of the paper is organized as follows. We provide the problem description in section 2, together with the relevant data. Section 3 concerns the Resource-Task Network (RTN) representation of the process, with emphasis on the modeling of the alternative operating modes for the electric arc furnaces and the electrode replacement tasks. The discrete-time RTN formulation is the subject of section 4, where we consider two alternative objective functions, both including the minimization of electricity and electrode replacement cost. Section 5 discusses the computational results, with emphasis on identifying the optimal operating modes for a given electricity price profile and condition of the electrode system. Finally, the conclusions are given in section 6.

2. Problem Statement

We consider the short-term scheduling problem of the melt shop production process of a steel plant under hourly changing electricity pricing, known ahead of time. The process under consideration can be classified as a flexible flowshop with four production stages, as seen in Figure 1, each with two units in parallel. Minimum and maximum transfer times between consecutive stages are given in Table 1.
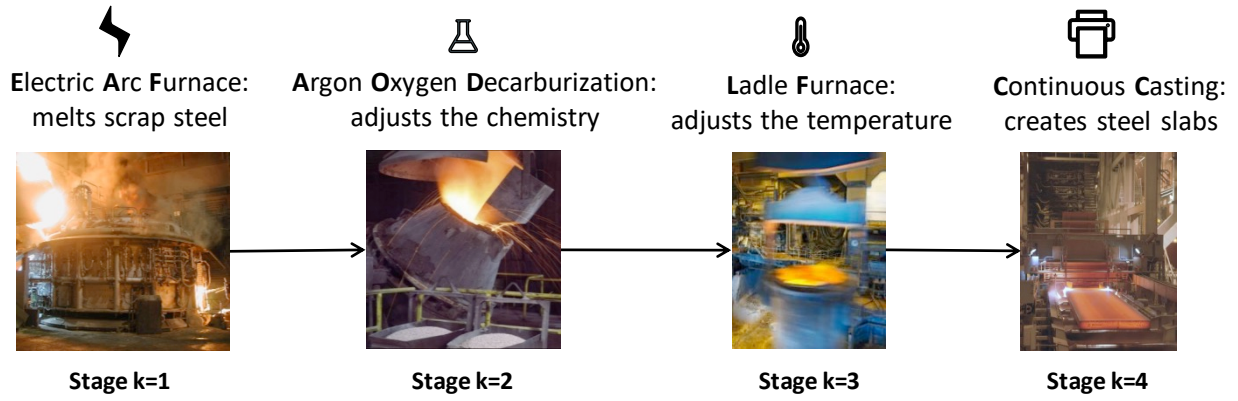
Figure 1. The melt shop consists of four production stages

Table 1. Minimum trf_k^L and maximum trf_k^U transfer times to stage k (min)

Stage	$k=2$	$k=3$	$k=4$
trf_k^L	10	4	10
trf_k^U	240	240	120

Table 2. Processing times (min) in Argon Oxygen Decarburization units, Ladle Furnaces and Continuous Casters (for Electric Arc Furnaces see Table 5).

Steel heat/Unit	AOD_{1-2}	LF_{1-2}	CC_1	CC_2
H_1-H_4	75	35	50	50
H_5-H_6	80	45	60	60
H_7-H_8	80	20	55	55
H_9-H_{12}	95	45	60	60
H_{13}-H_{14}	85	25	70	70
H_{15}-H_{17}	85	25	75	75
H_{18}	95	45	60	60
H_{19}	95	45	70	70
H_{20}	95	30	70	70
H_{21}-H_{22}	80	30	50	50
H_{23}-H_{24}	80	30	50	60

As a case study, we assume the production of 24 specific steel heats over a 24-h time horizon. In the first three stages, the processing time of heat h does not depend on the unit, while the duration in the continuous casters is slightly different for heats H_{23}-H_{24}, as seen in Table 2. As detailed in ref. 21, heats with similar grade characteristics form casting sequences that need to be processed uninterruptedly (check Table 3 for the correspondence between groups and steel heats). At the end of

the casting sequence, there is a changeover time of 70 min for CC_1 and 50 min for CC_2. The power consumption in stages two to four is given in Table 4.

The first stage is the most energy intensive and concerns melting in an electric arc furnace (EAF). It is assumed that the electric power consumption is constant throughout the duration of the melting task and that there are three alternative operating modes to choose from, M_1-M_3, ranging from low to high power intensity (check values in Table 5). One can see that increasing the power consumption reduces the duration of the task, giving more options to the scheduler to take advantage of periods of low electricity pricing, but decreases both energy efficiency and the lifetime of the electrodes. It should be highlighted that there is no need to consider more modes, with only slight differences in power consumption and duration, since we need to use slots of size $\delta = \{5,10,15\}$ min to ensure tractability of the discrete-time formulation, and the alternative durations need to be dissimilar when rounded up to a multiple of δ.

Table 3. In the continuous casters, steel heats are processed in six groups

Group g	G_1	G_2	G_3	G_4	G_5	G_6
H_g	H_1-H_4	H_5-H_8	H_9-H_{12}	H_{13}-H_{17}	H_{18}-H_{20}	H_{21}-H_{24}

Table 4. Power consumption pw_k in Argon Oxygen Decarburization units, Ladle Furnaces and Continuous Casters (MW)

Stage	$k=2$	$k=3$	$k=4$
pw_k	2	2	7

The electrode system of the electric arc furnace consists of a pile of several electrodes. A new electrode has $mass = 1180$ kg and costs $c^{RE} = $ €20,000. As the current is run through the electrodes to melt the steel, they sublimate due to the high temperatures. When the mass of the bottom electrode is totally consumed, a new electrode must be inserted at the top of the pile for the production to continue, as illustrated in Figure 2. Notice that the darker electrode may already have suffered some

degradation from the last batch (steel heat) when the electrode replacement task of 30 min is executed. Based on the values in Table 5, we set such mass tolerance to Δm=123 kg.

Table 5. Alternative operating modes in Electric Arc Furnaces (stage $k = 1$)

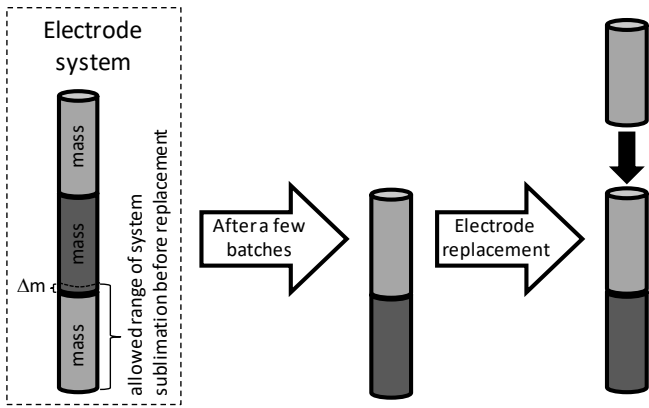| Operating mode m	M_1	M_2	M_3
Power consumption $pw_{k=1,m}$ (MW)	40	60	75
Duration for steel heats H_1-H_8, H_{13}-H_{17}, H_{21}-H_{24} (min)	69	49	41
Duration for steel heats H_9-H_{12}, H_{18}-H_{20} (min)	76	54	45
Electrode mass consumption $ma_{h,m}$ for H_1-H_8, H_{13}-H_{17}, H_{21}-H_{24} (kg)	123.3	131.4	137.4
Electrode mass consumption $ma_{h,m}$ for H_9-H_{12}, H_{18}-H_{20} (kg)	135.7	144.5	151.2

Figure 2. Electrode replacement in electric arc furnaces.

The objective is to minimize the total operating cost, consisting of electricity and electrode material costs. It should be highlighted that despite being of the same order of magnitude, the latter cost has previously been neglected.

3. Resource-Task Network representation of the system

Castro et al.[21] tackled a closely related scheduling problem from the same steel plant with a discrete-time formulation based on the RTN process representation[22]. Since many features are shared with the RTN presented next, here we only focus on the differences resulting from considering alternative operating modes for the electric arc furnaces and electrode replacement tasks.

In a discrete-time RTN formulation, equipment units can be treated as identical if their tasks have the same duration and involve the same consumption/production of resources. In such case, two

identical parallel units can be modeled as an aggregate unit of size 2, to improve computational performance by reducing symmetry. From the problem statement in section 2, we know that the processing times and power requirements for the first three production stages only depend on the steel heat, so the EAFs, AODs and LFs can potentially be treated as aggregate units. Unfortunately, to accurately model electrode degradation, we need to treat the electric arc furnaces individually. Thus, stages $k=2$ and $k=3$ consider aggregate equipment units of size two, information provided by the following initial availability parameters: $R^0_{AODs}=R^0_{LFs}=2$; while stages $k=1$ and $k=4$ feature two individual units ($R^0_{EAF_1}=R^0_{EAF_2}=R^0_{CC_1}=R^0_{CC_2}=1$).

In stage 1 in Figure 3, the melting tasks of a steel heat produce, at the end of execution, the sequential resource that locates the heat at the exit of the electric arc furnaces (e.g. H_1_E for heat H_1). These resources need to be consumed as soon as they are produced, meaning that the corresponding transfer task (Transfer_H_1_E_A) needs to start immediately after the end of the melting task. Its duration, Duration_E_A, is set to the minimum transfer time to stage 2, $trf^L_{k=2}$ (check Table 1). The transfer task takes the heat to the entrance of the Argon Oxygen Decarburization units, generating resource H_1_A^i. At this state, the steel heat can wait for $trf^U_2 - trf^L_2$ minutes until the start of the second stage of production. The same constraints are enforced for all other stages' output (e.g. H_1_A^o and H_1_L^o) and input location resources $r \in R^{IL}_{h,k}$ (e.g. H_1_L^i and H_1_C).

The last three stages of production have a single operating mode (check processing times in Table 2 and Table 4, respectively). Notice that the casting tasks, unlike the processing tasks of the previous stages, are defined for a group g of heats (e.g. $G_1 = \{H_1, H_2, H_3, H_4\}$). Although not apparent from Figure 3, they need to be executed uninterruptedly, in an ordered sequence that includes a changeover time at the end (see details in ref. 21). The output from the final production stage are the final product resources, e.g. H_1.
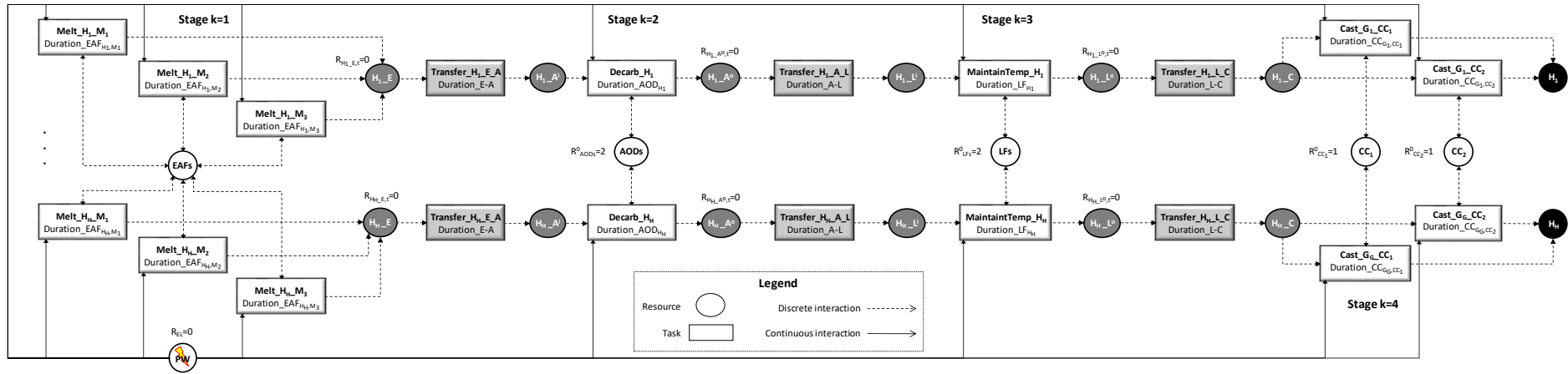
Figure 3. Resource-Task Network process representation showing three alternative operating modes for melting the steel heats in the electric arc furnaces. Note that we show fewer tasks and resources than those needed for modelling stage k=1, to emphasize that alternative operating modes can be handled by using one aggregate unit (named here as EAFs), when dealing with unit independent processing times (within a stage). However, due to the explicit modelling of the electrode system (Figure 4), we will need to use individual units for the furnaces: EAF_1 and EAF_2.

Most interactions of resources with tasks occur either at the beginning or at the end of task execution. They are represented in Figure 3 in the form of dashed lines, with double arrows indicating a temporary consumption of the resource (equipment units are regenerated at the end of the tasks). In contrast, the consumption of electrical power PW occurs throughout the duration of the processing task. To make a distinction, such continuous interaction is represented by a solid line.

3.1. Alternative operating modes in EAFs

In the presence of alternative operating modes for the electric arc furnaces, we need to replicate the melting task of a steel heat into as many copies as the number of operating modes. Note, however, that the copies are not exact since each has a different power consumption that is reflected into a shorter or longer duration. In Figure 3, we show the required tasks for the first H_1 and last H_H steel heat, where $m \in \{M_1, M_2, M_3\}$ represents the operating mode. As an example, Melt_H$_1$_M$_1$, with a duration Duration_EAF$_{H1,M1}$ (see Table 5), represents the processing task of H_1 in mode M_1. All melting tasks temporarily use an electric arc furnace.

3.2. Electrodes degradation in electric arc furnaces

Electrode replacement is a relevant part of the operating cost of electric arc furnaces. Electrode sublimation rate is a function of power consumption, with the benefits of a shorter processing time resulting from a higher power consumption being counteracted by a slightly greater electrode mass depletion. It may force electrode replacement after a smaller number of batches, during which the electric arc furnace will be inoperative. We thus need to take into consideration the state of the electrode when generating the schedule, to accurately compute the operating cost.

Since each electric arc furnace has its own electrode system, we cannot consider the two furnaces as an aggregate resource to model electrode degradation. Let resource Elect$_1$ represent the electrode system of electric arc furnace EAF$_1$. The initial condition at the beginning of the time horizon if given by $R^0_{Elect_1}$, which can be the electrode mass when new, given by parameter $mass$. Melting consumes

a certain mass of electrode, a value that is a function of the steel heat and the operating mode (recall Table 5). In the context of a discrete-time RTN formulation, it can be modeled through structural parameters $\mu_{r,i,\theta}$ that define the amount of resource r consumed/produced by task i at a time θ relative to the start of the task. More specifically, and being parameter $ma_{h,m}$ the mass required to process heat h in mode m, making $\mu_{Elect_1,H_1\_EAF_1\_M_1,0} = -ma_{H_1,M_1}$ forces the consumption at the beginning of the processing task of heat H_1 in EAF_1 operating in mode M_1, of the needed electrode mass of $Elect_1$. In other words, the task can only start if enough mass is available.

Figure 4 shows the value of all non-zero structural parameters dealing with resources of equipment units, electrodes and the sequential resource (H$_1$_E) for the first steel heat. Notice that electric arc furnace EAF_2 is consumed at the start of all tasks i of type Melt_H$_1$_EAF$_2$, i.e. $\mu_{EAF_2,i,0} = -1$. The equipment resource is then produced at the end of task, which occurs at a time $\tau_{H_1,m}$ relative to the start of the task, where m is the operating mode. The required parameter for mode M_2 is thus $\mu_{EAF_2,H_1\_EAF_2\_M_2,\tau_{H_1,M_2}} = 1$. Resource H$_1$_E is also produced at the end of the task: $\mu_{H_1\_E,H_1\_EAF_2\_M_2,\tau_{H_1,M_2}} = 1$.

The electrode replacement tasks in Figure 4, e.g. ReplaceElect_EAF$_1$, have the purpose of adding a new electrode, which is done simply by producing the amount $mass$ at the end of the 30 min duration. The required parameter for EAF_1 is: $\mu_{Elect_1,Rep\_EAF_1,\lceil 30/\delta \rceil} = mass$.

It should be highlighted that the modeling of electrode degradation resembles that of decreasing processing capacity in the extended RTN formulation of Nie et al.[26]. In both formulations: (i) the amount of capacity resource consumed depends on the decisions taken by the optimization, either the processing rates of the continuous tasks[26] or the operating modes of the batch tasks; (ii) the condition of the unit does not affect performance, unless it is below the threshold that prevents operation. The most significant difference is that in Nie et al.[26], the replenishment task brings the unit back to full capacity regardless of the initial condition, whereas in the current work, the electrode masses before and after maintenance are related, which is simpler to model.
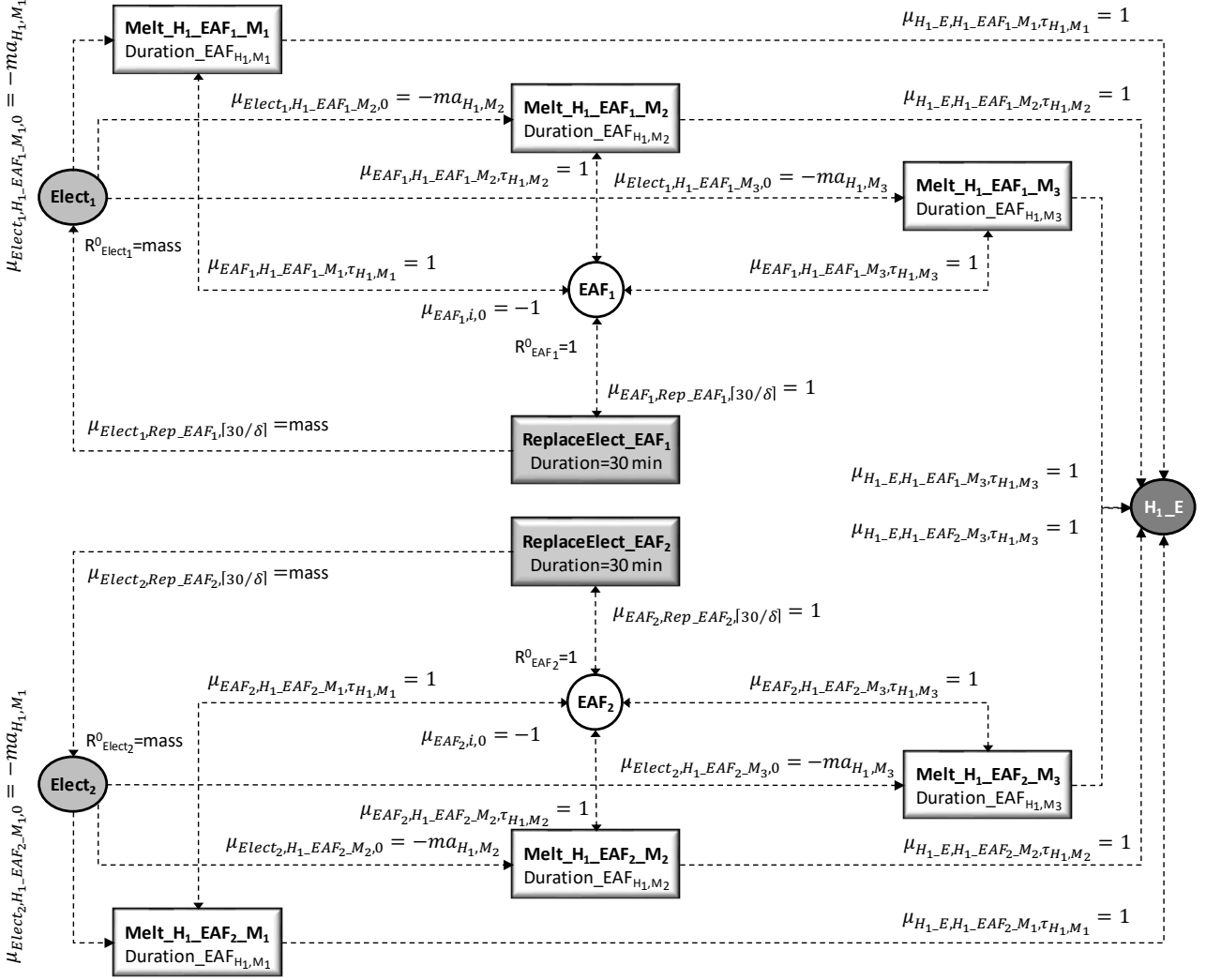
Figure 4. Resource-Task Network process representation handling electrode degradation in the electric arc furnaces operating in one of three alternative modes, for steel heat H_1.

4. Mathematical Formulation

The structural parameters of the RTN are used to transform a generic formulation into one that is specific to the scheduling problem at hand. In this section, we present the constraints that are needed to accurately model the system, ensure that all heats reach the condition of final product, and achieve good computational performance (based on experience). We also discuss the time representation used by the model and two closely related objective functions.

4.1. Discrete-time representation

To keep track of scheduling events, we rely on a single, 24-h time grid that is discretized into uniform slots $t \in T$ of size δ (min), as seen in Figure 5. To accurately account for the electricity cost with prices that change every hour, we assume that 60 (min) is a multiple of δ. The mathematical formulation to be presented next works with time slots, so all durations d_i given in section 2, in minutes, need to be converted into a number-of-time-slots basis τ_i. To ensure feasibility of the schedule, durations are rounded up to a multiple of δ: $\tau_i = \lceil d_i/\delta \rceil$, where $\lceil \quad \rceil$ is the ceiling function.
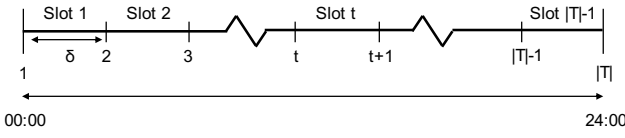

Figure 5. Underlying uniform discrete-time grid.

4.2. Model variables

The mathematical formulation uses a single set of binary variables, $N_{i,t}$, which assign the start of task i to the start of slot t. Since we are dealing with a multistage process, it is possible to reduce the domain for task execution after computing earliest starting and finishing times for processing and transfer tasks (see for instance Castro et al.[34]). In contrast, we consider the full time-domain for electrode replacement tasks, to allow for different conditions in terms of initial electrode mass. The slots at which task i can start are the elements of subset T_i.

Nonnegative continuous variables $\Pi_{r,t}$, compute the power $r \in R^{PW}$ (MW) and energy $r \in R^{EN}$ (MWh) that needs to be purchased from electricity markets during slot t. If processing task i requires an amount pw of power, then it will consume such value in every slot where it is active, i.e. $\mu_{r,i,\theta} = -pw \; \forall r \in R^{PW}, \theta \in \{0, \ldots, \tau_i - 1\}$. However, whenever there are rounding errors in the processing times, the power consumption will not be constant during the last active slot. To accurately compute

the energy consumption (and then the cost), we use the energy resource instead, only accounting for

the active part of the task, i.e. $\mu_{r,i,\theta} = \begin{cases} -\frac{pw \cdot \delta}{60} & if \ \theta \in \{0, \dots, \tau_i - 2\} \\ -\frac{pw \cdot (\delta + d_i - \delta \cdot \tau_i)}{60} & if \ \theta = \tau_i - 1 \end{cases} \ \forall r \in R^{EN}.$

While we just consider the day-ahead spot market, with hourly varying prices assumed to be known

a few hours ahead, it is straightforward to define one energy resource per energy market. Specifically,

the electricity purchase options in Hadera et al.[15], include a long-term contract with a fixed amount

of electricity at a fixed price, short-term time-of-use contracts with on- and off-peak prices (known

in advance), day-ahead, and onsite generation at a constant price but with start-up costs. In Castro et

al.[21], we show how to compute deviations from a precontracted load curve, which could lead to

interaction with the intraday or real-time markets. The interested reader in developing a framework

to determine optimal electricity market participation strategies for individual participants may also

find useful the work of Dowling et al.[35].

Continuous variables $R_{r,t}$ represent the excess value of resource r at the start of slot t. They assume

nonnegative values for all non-electrode resources, i.e. $R_{r,t} \geq 0 \ \forall r \notin R^{EM}, t$. For electrode resources,

the excess values can take negative values, in the range: $-\Delta m \leq R_{r,t} \leq mass \ \forall r \in R^{EM}, t$. Setting

$R_{r,t} = 0 \ \forall t$ is mandatory for some resources. As mentioned in section 3, we do it for the outlet

resources of stages 1-3, to ensure immediate execution of the transfer tasks, and for the energy and

power resources ($r \in R^{PW} \cup R^{EN}$).

4.3. Objective functions

We consider two objective functions that share the total energy and electrode replacement cost

terms. Total energy cost is computed by multiplying the electricity price $price_{hr}$, by the sum of the

energy consumed in all slots t belonging to hour hr ($t \in T_{hr}$; easy to compute as a function of δ).

The electrode replacement cost is incurred by executing electrode replacement tasks $i \in I^{RE}$.

However, the second term in eqs. (1)-(2) is insensitive to the number of batches left in the electrodes

at the end of the time horizon, which may be important. The last term in eq. (2) makes the replacement cost continuous by also accounting for the fraction of electrode $r \in R^{EM}$ that has been consumed (positive term) or produced (negative term). It is computed by dividing the difference between the electrode condition at the beginning of the time horizon R_r^0 and the final electrode mass $R_{r,|T|}$, by the mass of a new electrode.

$$\min \sum_{r \in R^{EN}} \sum_{hr} price_{hr} \sum_{t \in T_{hr}} \Pi_{r,t} + c^{RE} \sum_{i \in I^{RE}} \sum_{t \in T_i} N_{i,t} \tag{1}$$

$$\min \sum_{r \in R^{EN}} \sum_{hr} price_{hr} \sum_{t \in T_{hr}} \Pi_{r,t} + c^{RE} \sum_{i \in I^{RE}} \sum_{t \in T_i} N_{i,t} + \frac{c^{RE}}{mass} \sum_{r \in R^{EM}} (R_r^0 - R_{r,|T|}) \tag{2}$$

4.4. Model constraints

The excess resource balances are the most important set of constraints for any RTN formulation since they collect the information of the RTN superstructure in an elegant way. In eq. (3), the excess of resource r at time t, $R_{r,t}$, is related to the amounts produced/consumed by all tasks ending/starting at t and either to its value at t-1, $R_{r,t-1}$, or to the amount purchased from outside during slot t, $\Pi_{r,t}$.

$$R_{r,t} = R_r^0|_{t=1} + R_{r,t-1}|_{t>1, r \notin (R^{PW} \cup R^{EN})} + \Pi_{r,t}|_{r \in (R^{PW} \cup R^{EN})} + \sum_i \sum_{\substack{\theta=0: \\ t-\theta \in T_i}}^{\tau_i} \mu_{r,i,\theta} N_{i,t-\theta} \ \forall r, t \tag{3}$$

In eq. (3), energy and power resources ($r \in R^{PW} \cup R^{EN}$) are treated in a different manner from the others. To prevent the purchase of more low-cost energy than needed by active tasks (we have no means of storing energy to be used at a later time), we eliminate the connection with the resource values at $t - 1$. Coupled with $R_{r,t} = 0$ (as stated in section 4.2), it leads to the simplification of the constraint to $\Pi_{r,t}|_{r \in (R^{PW} \cup R^{EN})} = -\sum_i \sum_{\theta=0: t-\theta \in T_i}^{\tau_i} \mu_{r,i,\theta} N_{i,t-\theta}$, which reflects that all energy purchased from the market during slot t must be consumed by tasks starting at t (note that $\mu_{r,i,0} < 0$).

For the outlet resources of stages 1-3, we fix $R_{r,t} = 0 \ \forall t$, and so eq. (3) becomes: $\sum_i \sum_{\theta=0: t-\theta \in T_i}^{\tau_i} \mu_{r,i,\theta} N_{i,t-\theta} = 0$. Therefore, if the resource is produced by task i at time t, meaning $N_{i,t-\tau_i} = \mu_{r,i,\tau_i} = 1$, then, a resource consuming task i' must start at t, i.e. $N_{i',t} = 1$ and $\mu_{r,i',0} = -1$.

With the excess resource balances in eq. (3), it is still possible for the electrode replacement task $i \in I_r^{RE}$ of electrode r, to start while there is still some residual electrode mass left, $mass^R$. This, provided that the subsequent melting task, which subtracts $ma_{h,m}$, starts immediately after, and that $ma_{h,m} \geq mass^R$. To ensure that a replacement task, which will add $mass$ to the value of the corresponding $R_{r,t}$ variable at $t + \tau_i$ (check Figure 4), only starts after the electrode mass reaches zero or a negative value, we use eq. (4).

$$R_{r,t} + \sum_{i \in I_r^{RE}} \mu_{r,i,\tau_i} N_{i,t} \leq mass \ \forall r \in R^{EM}, t \tag{4}$$

The next two sets of constraints ensure that every steel heat h is processed exactly once on stage k. The difference between eqs. (5)-(6), is that last-stage heats are hidden in groups g, recall Table 3. Note that subset $I_{h,k}$ holds the processing tasks of heat h belonging to stage k, while I_g identifies the casting tasks of group g.

$$\sum_{i \in I_{h,k}} \sum_{t \in T_i} N_{i,t} = 1 \ \forall h, k = 1, \dots, 3 \tag{5}$$

$$\sum_{i \in I_g} \sum_{t \in T_i} N_{i,t} = 1 \ \forall g, k = 4 \tag{6}$$

For the steel heats to reach the different stages, the transfer tasks must also be executed. In eq. (7), subset $I_{h,k}^T$ holds the transfer task of heat h from stage k to stage $k+1$.

$$\sum_{i \in I_{h,k}^T} \sum_{t \in T_i} N_{i,t} = 1 \ \forall h, k \leq 3 \tag{7}$$

Finally, we need to ensure that the maximum transfer time between stages is not exceeded. For the inlet location resource $r \in R_{h,k}^{IL}$ of heat h to stage k, this is done by limiting the number of slots with $R_{r,t}=1$, to the difference between the maximum and minimum transfer times (note that we subtract trf_k^L since this was set as the duration of the transfer task to stage k, as discussed in section 3). To make sure that the effect of the rounding errors is eliminated, we use the floor function $\lfloor \ \ \rfloor$ in eq. (8).

$$\sum_{r \in R_{h,k}^{IL}} \sum_t R_{r,t} \leq \left\lfloor (trf_k^U - trf_k^L)/\delta \right\rfloor \ \forall h, 1 < k \leq 4 \tag{8}$$

5. Computational Results

The mixed-integer linear programming model was implemented in GAMS 26.1 and solved with CPLEX 12.8 running in parallel deterministic mode using up to eight threads. Default settings were used except for the maximum wall time limit of one hour. Since all optimization runs in the following tables ended with this criterion, we just report the optimality gap at termination. The hardware consisted of a Windows 10, 64-bit desktop computer with an Intel i7-4790 (3.6 GHz) processor and 8 GB of RAM.

We have used the electricity prices in Table 6, representative values from the EPEX day-ahead spot market, and assume that both electrodes have just been replaced before the beginning of the time horizon, i.e. $R_r^0 = mass \; \forall r \in R^{EM}$. Over the next couple of sections, we discuss the results for the two alternative objective functions given in eqs. (1) and (2).

Table 6. Hourly Electricity prices (€/MWh) for sections 5.1 to 5.3 and 5.5. Taken from www.epexspot.com/en/market-data/dayaheadauction, former DE/AT market).

Hour hr	0:00	1:00	2:00	3:00	4:00	5:00	6:00	7:00	8:00	9:00	10:00	11:00
$price_{hr}$	40.84	41.15	43.77	39.97	40.81	43.04	45.37	49.49	59.92	60	60.04	57.7
Hour	12:00	13:00	14:00	15:00	16:00	17:00	18:00	19:00	20:00	21:00	22:00	23:00
$price_{hr}$	52.86	50.05	50.94	54.04	57.52	64.91	59.92	57.99	43.68	38.46	40.94	35.89

5.1. Discrete electrode replacement cost

The objective function in eq. (1) minimizes the total operating cost considering a discrete electrode replacement cost. By discrete, we mean that the objective function is insensitive to the condition of the electrodes at the end of the 24-h scheduling period, costing the same to end with a barely used electrode or a depleted one. This is not good for the linear relaxation of the model since the optimization solver will be able to execute the replacement tasks partially, to regenerate the minimum amount of mass needed to process the 24 steel heats. Listed in Table 7 are the results as a function of the slot size, $\delta=\{5, 10, 15\}$ min, where it can be seen that CPLEX is unable to find a feasible solution for the finest grid setting and that the best solution is obtained for $\delta=10$ min.
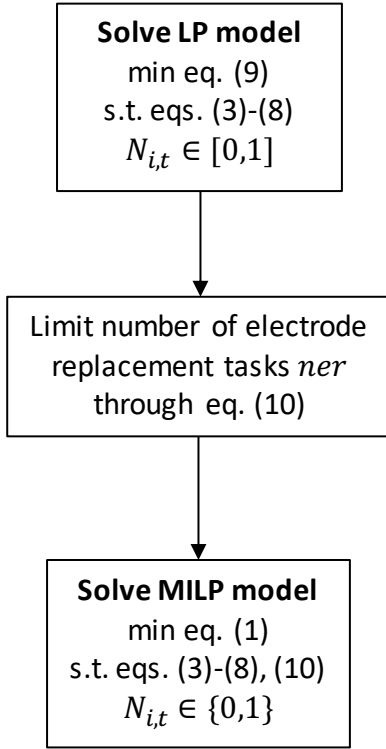
19

Figure 6. Two-stage procedure for reducing the integrality gap when working with a discrete replacement cost in the objective function.

Table 7. Results for objective function with discrete electrode replacement cost.

δ (min)	EAF modes	MILP (€)	LP relaxation (€)	Optimality gap
15	(M_1,M_2,M_3)	87,001	75,377	13.3%
10	(M_1,M_2,M_3)	86,827	73,718	15.1%
5	(M_1,M_2,M_3)	no solution	73,671	-

One way to significantly reduce the integrality gap, is to limit the number of electrode replacement tasks. This can be done systematically by means of the two-stage procedure illustrated in Figure 6. The number of replacements, ner, can be quickly estimated by solving the linear relaxation problem (LP) of the basic MILP formulation with eq. (9) replacing eq. (1) as the objective, and rounding up the solution to the next integer. One can then go back to the MILP, adding eq. (10) and returning to eq. (1) as the objective. Note that we use $\geq$ in eq. (10) since the equality is not guaranteed to lead to a feasible MILP. This was observed experimentally, after fixing $ner=1$ for an instance with an LP solution equal to 0.991.

$$\min \sum_{i \in I^{RE}} \sum_{t \in T_i} N_{i,t} \tag{9}$$

$$\sum_{i \in I^{RE}} \sum_{t \in T_i} N_{i,t} \geq ner \tag{10}$$

Table 8. Results for objective function with discrete electrode replacement cost and 2-stage solution procedure.

δ (min)	EAF mode	MILP (€)	LP rel. (€)	Opt. gap	# heats in (M_1,M_2,M_3)	Binary variables	Total variables	Equations
15	(M_1,M_2,M_3)	86,894	86,297	0.61%	(15,2,7)	19661	37122	17684
10	(M_1,M_2,M_3)	85,730	85,210	0.57%	(11,12,1)	30067	56168	26324
5	(M_1,M_2,M_3)	85,774	85,153	0.71%	(12,8,4)	60924	112945	52244

The results in Table 8, which are not guaranteed to be the global optimum, show that we were able to reduce the integrality gap by roughly one order of magnitude, leading to reasonable optimality gaps at termination (below 1%). More importantly, we have been able to find a good feasible solution for δ=5 min, and to reduce the cost of the best-found solution by 1.26%, from €86,827 to €85,730. This is shown in Figure 7 and described next.

The first stage of the solution procedure for δ=10 min, returns a value of 0.3729, indicating the need to replace one electrode, at least. Looking at the optimal solution from the second stage of the procedure, it starts shortly after 11:00 (black rectangle in Figure 7) and is allocated to EAF$_2$. It occurs three hours later than the end of the melting task in orange (heat H$_{20}$), which took the electrode mass to -52.9 kg. Interestingly, the two EAFs follow very different strategies during the first 8 hours of operation, despite starting with the same mass, 1180 kg. EAF$_2$ selects shorter tasks, being able to process 9 heats vs. 7 of EAF$_1$, in which all but two correspond to a mid-power (M$_2$) intensity mode. The consequence is the sharper decrease in mass compared to EAF$_1$, which saves 263.5 kg to later process heats H$_6$ and H$_{23}$ in the most energy efficient mode M$_1$, when the cost is around 51 €/MWh, and H$_8$ in M$_2$, when electricity is cheaper (43.68 €/MWh). Note that since EAF$_1$ ends operation around 21:00, with the electrode in a condition of -114.5 kg, it would have made sense to execute the expensive replacement task immediately after, to make the furnace ready for the next scheduling

period (see recent work of Lee et al.[36] on how to generate alternative schedules in the context of a rolling horizon approach).
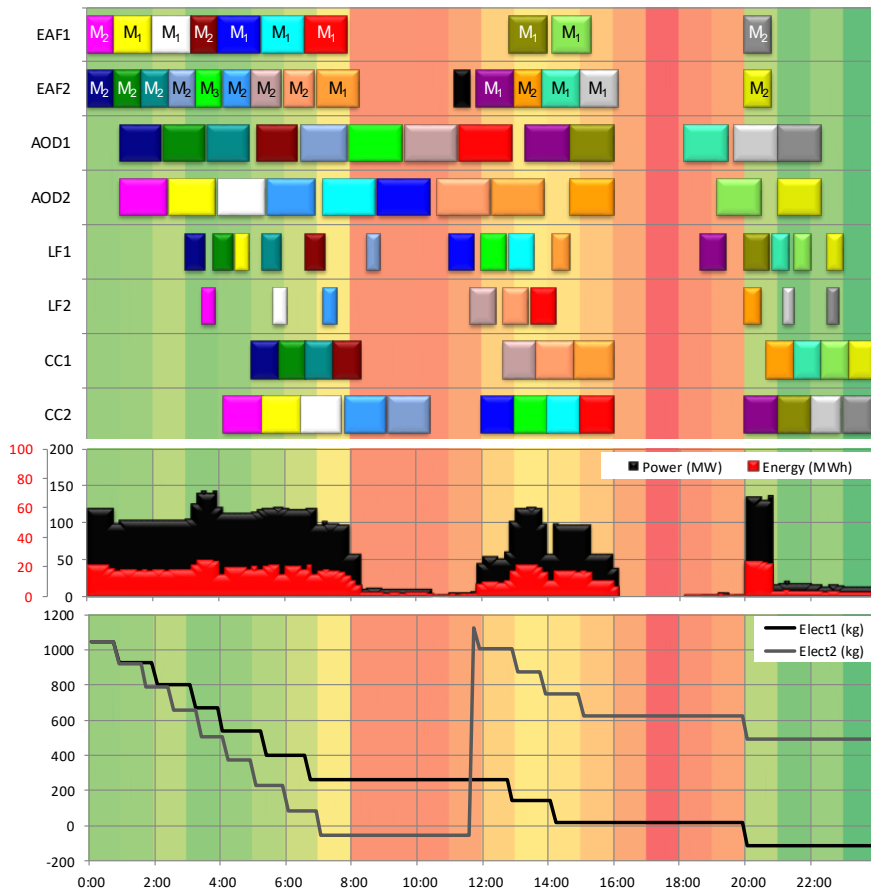

Figure 7. Best-found solution (€85,730) when considering discrete electrode replacement cost in the objective function (δ =10 min). Note that background colors are related to hourly electricity prices (lowest for dark green and highest for dark rose).

The main contributor to the objective function is, however, the electricity cost and so the schedule should avoid production when electricity is more expensive. To facilitate the analysis of the schedule, the background of Figure 7 feature colors that are related to the electricity price, ranging from the cheapest prices in dark green to the most expensive in dark rose. It is clear that the EAFs avoid operation in the rose periods. Since EAFs perform by far the most energy intensive tasks, it is not surprising that the power and energy profiles reach values close to zero in such periods.

Overall, 11 steel heats are processed in low-power mode M_1, 12 in M_2 and 1 in high-power mode M_3. The optimization can thus take full advantage of the flexible operating modes for the electric arc furnaces.

5.2. Continuous electrode replacement cost

The objective function in eq. (2) considers a continuous replacement cost, i.e. we account for the cost of purchasing new electrodes but also penalize the decrease in mass compared to the initial condition. Changing the objective function neither affects the feasible region of the MILP nor its LP relaxation but has the advantage of leading to a lower integrality gap. Therefore, the heuristic procedure in Figure 6 is no longer required. The total operating cost in Table 9 becomes 38% higher than the values in Table 8 and heats are no longer processed in high-mass consumption mode M_3. The other result worth highlighting are the lower optimality gaps. Note that the errors from rounding the processing times are higher for $\delta = 10$ than for $\delta = 5$, meaning fewer options to take advantage of lower electricity prices. Thus, the solution from the MILP should not degrade with decreasing δ, unless we are unable to solve the problem to optimality (if we account for the optimality gaps, the best possible solution at termination is lower for $\delta = 5$).

Table 9. Results for objective function with continuous electrode replacement cost.

δ (min)	EAF mode	MILP (€)	LP relaxation (€)	Opt. gap	# heats in (M_1, M_2, M_3)
15	(M_1, M_2, M_3)	119,886	119,547	0.23%	(21,3,0)
10	(M_1, M_2, M_3)	118,143	117,888	0.18%	(22,2,0)
5	(M_1, M_2, M_3)	118,260	117,840	0.33%	(21,3,0)

Figure 8 presents the best-found solution, where the most striking difference compared to Figure 7 is that the electrode mass profiles for the two EAFs are very similar. With the continuous replacement cost, the impact of replacement tasks is much lower, and therefore the optimization decides to execute two instead of one. As a consequence, the electrodes still have capacity for a few batches at the end of the day, not compromising the decision-making for the next 24 hours. Another advantage of this

schedule is that it keeps power consumption below 100 MW, except for the first 49 min, during the parallel processing of heats H_1 and H_{13} in mode M_2. Afterwards, all melting tasks are performed in low-power mode M_1. Since this is the mode with longer processing times, two melting tasks need to be shifted to the intermediate price periods between 11:00 and 17:00 (compared to Figure 7). Overall, the power and energy consumption profiles are smoother, which is better for the power grid.
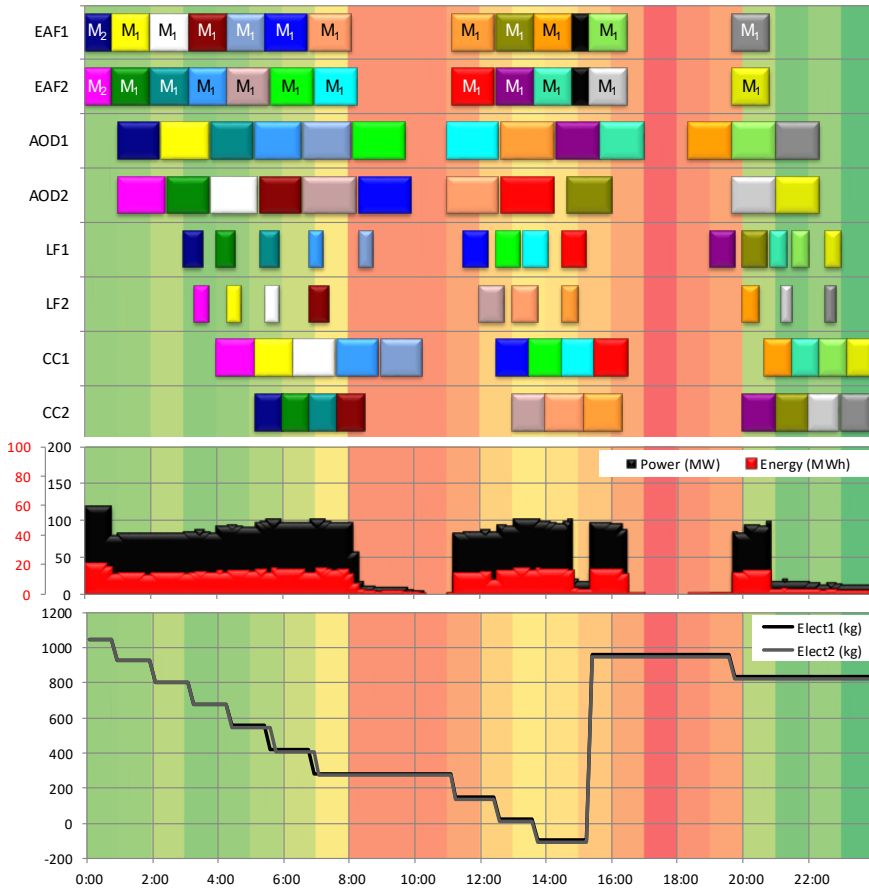

Figure 8. Best-found solution (€118,143) when considering continuous electrode replacement cost in the objective function (δ =10 min).

We thus conclude that the objective with continuous replacement cost is more appropriate and so it will be the only option considered in the remaining paper.

5.3. Alternative vs. single operating mode

With the proposed mathematical formulation, for every melting task performed in the Electric Arc Furnaces we have the option to choose the operating mode from three alternatives. From the analysis

of Table 10, we can see that the benefit can go up 7.22%. However, operating exclusively in low-power mode M_1 leads to essentially the same solution. The observed trend is that the lower the energy intensity mode the better. Thus, there is a clear trend for efficiency, both in terms of energy and electrode consumption, over production speed. Going for a single operating mode has the advantage of reducing problem size (by 35 and 18% in the number of binary and total variables, respectively), which may speed up solution time. Indeed, for M_1, the MILP problem for δ=15 min can be solved to optimality in 2724 CPUs (results not part of Table 10).

Table 10. Results for continuous replacement cost when considering a single operating mode for the EAFs (δ=10 min).

Mode	Cost (€)	Cost Increase	Opt. gap	Binary variables	Total variables	Equations
M_1	118,146	0.00%	0.10%	19342	45443	26323
M_2	122,089	3.34%	0.76%	19702	45803	26323
M_3	126,675	7.22%	0.88%	19755	45856	26323

5.4. Influence of electricity price profile

Electricity price is a major source of uncertainty for daily operation, and thus it is interesting to analyze the results for a different profile. After testing a few, we selected for illustration the profile benefiting multi-mode operation the most, which is given in Table 11. Compared to Table 6, the average price increased by 34% to 66.16 €/MWh, while the variance increased by almost two orders of magnitude. In particular, there is a steep rise from the minimum at 3:00 (35.1 €/MWh) to the maximum of 91.76 €/MWh at 9:00. Note that by raising the average electricity cost, we decrease the relative importance of the electrode cost term, increasing the likelihood of selecting modes with larger mass consumption.

The best-found solution for the profile in Table 11 is given in Figure 9. Compared to Figure 8, the optimization decides to finish the nightly operation of the furnaces sooner, while processing eight heats instead of seven on each EAF. This is accomplished by processing one heat in high-power mode

25

M_3 and nine more heats in medium-power mode M_2. It is important to highlight that the processing of the 12 heats in mode M_2 or M_3 occurs in the cheaper green region, where it pays to be faster, so that we can fit more tasks, and be less energy efficient. Notice also that the continuous caster units CC_1 and CC_2, belonging to the second most energy intensive stage, also avoid the dark-rose periods.

Table 11. Electricity price profile for section 5.4 (€/MWh). Taken from https://www.mercatoelettrico.org/En/Esiti/MGP, values for Italy, Monday 6/2/2017).

Hour hr	0:00	1:00	2:00	3:00	4:00	5:00	6:00	7:00	8:00	9:00	10:00	11:00
$price_{hr}$	43.31	41.4	38.27	35.1	36.3	42.49	55.98	74.95	88.93	91.76	90.98	91.46
Hour	12:00	13:00	14:00	15:00	16:00	17:00	18:00	19:00	20:00	21:00	22:00	23:00
$price_{hr}$	73.78	71.54	79.15	74.54	75.03	74.4	86.37	77.29	73.66	60.69	57.15	53.3

Table 12. Results for continuous replacement cost when considering a different electricity price profile (δ=10 min).

Modes	Cost (€)	Cost Increase	Opt. gap	# heats in (M_1,M_2,M_3)
(M_1,M_2,M_3)	132,783	-	0.67%	(12,11,1)
M_1	135,839	2.30%	0.11%	-
M_2	136,561	2.85%	1.42%	-
M_3	143,760	8.27%	3.66%	-

The results in Table 12 show that considering all three operating modes reduces the cost by more than €3000/day (2.30%). Like in Table 10, we observe the trend of the cost increasing with the power intensity, but this is not always valid. Results for the Tuesday, 24/01/2017, profile from the EPEX day-ahead spot market (average price doubled compared to Table 6), led to cost increments of 0.18% for medium-power mode M_2 and 3.76% for low-power mode M_1, despite the latter being once more the most selected in multimode operation (12 vs. 9 heats).
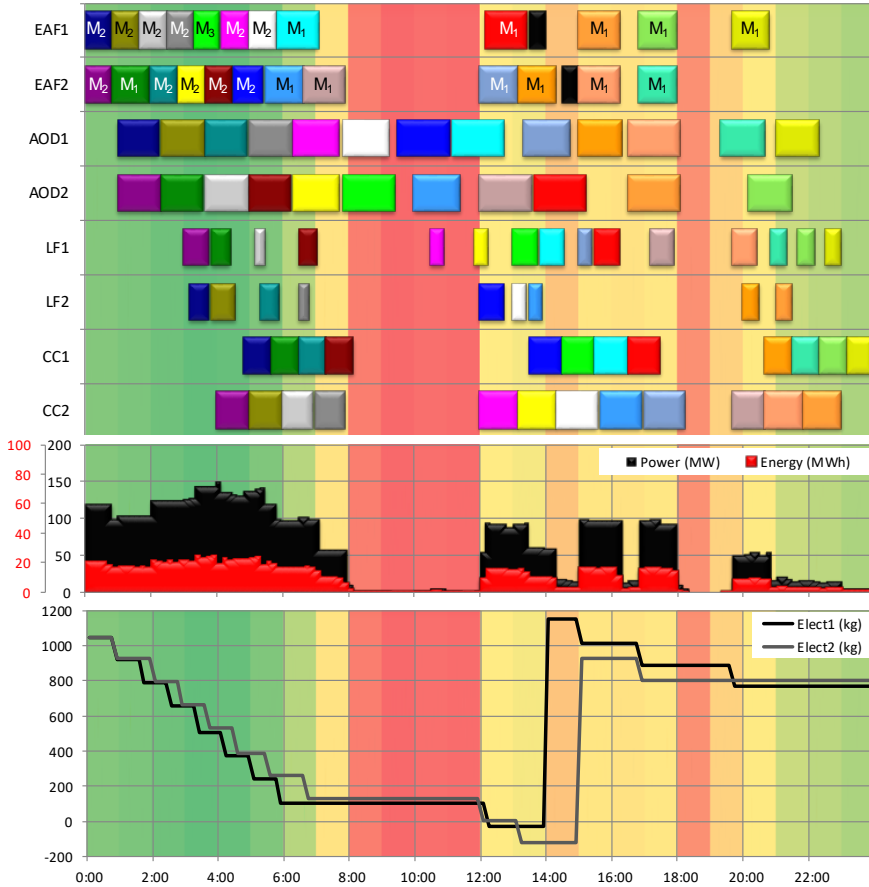
Figure 9. Best-found solution (€132,783) when considering continuous electrode replacement cost in the objective function and a different electricity price profile (δ =10 min).

5.5. Influence of initial electrode mass

All previous computational runs were made starting with new electrodes in the EAFs. We now study the influence of the initial electrode mass by considering R_r^0= 400 kg and 600 kg, for the $r \in R^{EM}$ resources of EAF$_1$ and EAF$_2$, respectively. In the bottom profiles of Figure 10, the values at 0:00 are lower, but this is because the melting tasks start at 0:00, leading to the immediate consumption of 131.4 kg in EAF$_1$ (H$_{13}$ in M$_2$) and 113.4 kg in EAF$_2$ (H$_1$ in M$_2$) and to excess resource values of 268.6 and 468.6 kg, respectively. Similarly, executing an electrode replacement task increases the mass by 1180 kg, but the maximum value in the chart is just above 1000 kg (for Elect$_2$) due to the immediate execution of heat H$_{10}$ in mode M$_1$, which deducts 135.7 kg. In other words, it is not easy to identify the start of a new batch in the furnaces just by looking at the stepwise graph (in this case, we have twenty steps for twenty-four heats).
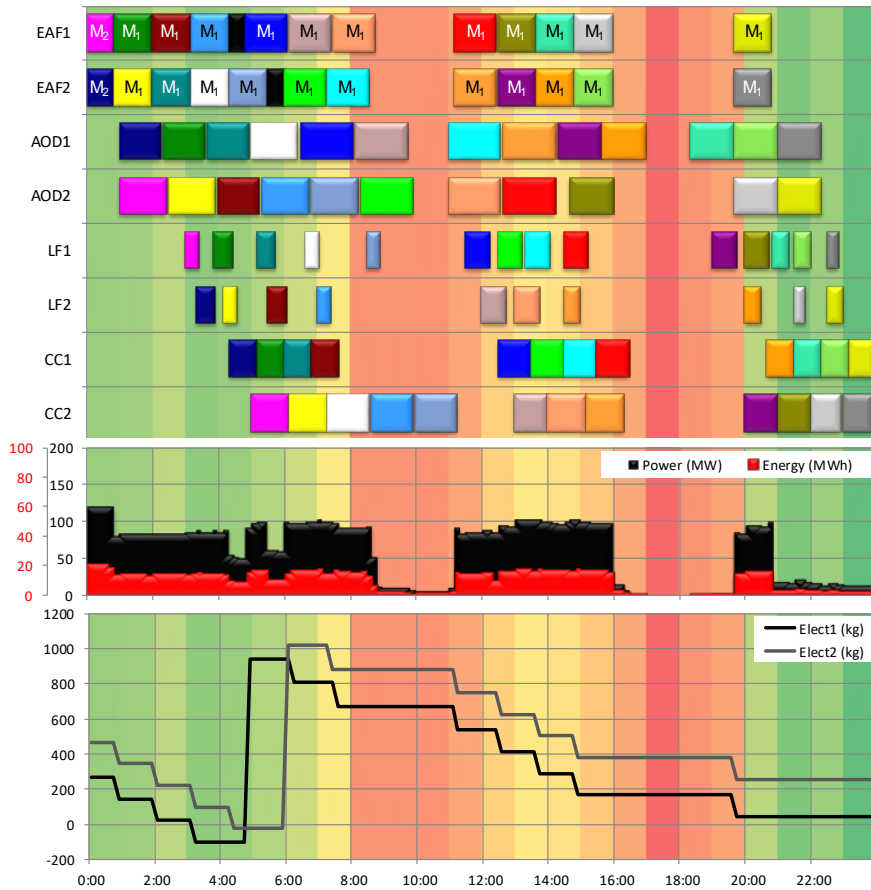
Figure 10. Best-found solution (€118,697) when considering continuous electrode replacement cost in the objective function and starting with used electrodes (δ =10 min).

Because of the lower initial mass, the electrode replacement tasks now need to be executed in the low-cost period (at 4:20 and 5:30), for the EAFs to still take advantage of the low electricity prices. Like in Figure 8, there are just two tasks executed in the medium-power mode and so the first period of operation (and maintenance) of the furnaces ends later, leading to a 0.47% increase in cost, to €118,697. Since the replacement tasks are not executed in parallel, there are two drops in electricity consumption rather than one sharp drop, but overall, the schedules in Figure 8 and Figure 10 are very similar.

6. Conclusions

This paper presented a mixed-integer linear programming formulation for generating the daily schedule of the melt shop of a steel plant purchasing electricity from the day-ahead spot market. The

novelty was to consider alternative operating modes for the electric arc furnaces together with the maintenance of their electrode systems, in order to achieve a tradeoff between energy efficiency, electrode lifetime and production time. Complicating scheduling constraints were derived after first representing the process as a Resource-Task Network.

We have shown the value of the new formulation for decision-making by optimally scheduling an order of 24 steel heats, for three different price profiles taken from day-ahead spot markets. Of the three specified operating modes, at least two were selected, with a preference for the low-power mode, which is the most energy efficient, consumes the least mass of electrode, but lasts the longest. Interestingly, we have seen that the low-power mode is not necessarily the best choice when restricting the plant to a single mode throughout the day. Overall, the benefits from multi-mode operation compared to just using the high-power mode, can exceed 8%.

The computational study also involved two objective functions, differing in the calculation of the electrode replacement cost, which is an important component of the total operating cost. While the cost only incurs when inserting a new electrode in the system, this discrete option drives the optimization to depleted electrodes towards the end of the 24-h scheduling horizon. Since this may compromise the schedule for the next period, and since electricity prices tend to be at the lowest earlier in the day, it is better to add a continuous term that accounts for the change of electrode mass between the beginning and the end (the initial electrode masses are model parameters). Still, the solution for 24 hours is only a first step to a realistic formulation where a longer horizon is considered (at least two days) and only the schedule for the first day is executed. The inclusion of the second day serves the purpose of avoiding strong cutoff effects, which can make the results suboptimal in the long run. This is similar to what is done in model-predictive control.

Alternative operating modes add flexibility to the system, but ideally one would want to change the mode during the melting of a steel heat and not just between heats. Furthermore, focusing exclusively

on the day-ahead energy market can significantly undervalue cost savings. These topics will be the subject of future work.

Acknowledgements

Nomenclature

Sets/Indices

g = group of steel heats
H_g = Steel heats belonging to group g
h = steel heat
hr = hour of the day
i, i' = processing, transfer or electrode replacement task
I_g = casting tasks of group g
$I_{h,k}$ = subset of processing tasks of heat h belonging to stage k
$I_{h,k}^T$ = subset of transfer tasks of heat h from stage k
I^{RE} = electrode replacement tasks
I_r^{RE} = electrode replacement task that regenerates electrode mass resource r
k = production stage
m = operating mode in electric arc furnace
r = resource
$R_{h,k}^{IL}$ = inlet location resource of heat h in stage k
R^{EN} = energy resource
R^{EM} = electrode mass resource
R^{PW} = power resource
T/t = time slots of discrete-time grid
T_{hr} = time slots belonging to hour hr
T_i = time slots where task i can start
θ = relative time with respect to the start of the task (ranges between 0 and τ_i)

Parameters

c^{RE} = cost of replacing an electrode (€)

d_i = duration of task i (min)

$ma_{h,m}$ = electrode mass degradation from processing heat h in operating mode m (kg)

$mass$ = electrode mass added to the system by electrode replacement task (kg)

$price_{hr}$ = price of electricity in hour hr (€/MWh)

$pw_{k,m}$ = power consumption in stage k operating in mode m, if relevant (MW)

R_r^0 = availability of resource r in the beginning of time horizon (used for equipment units and electrode mass resources)

trf_k^L / trf_k^U = minimum/maximum transfer time of every heat from stage k-1 to stage k (m³)

δ = size of every slot in discrete-time grid (min)

Δm = maximum mass degradation of second from bottom electrode before replacement task (kg)

$\mu_{r,i,\theta}$ = amount of resource r consumed (-) or produced (+) by task i at relative time θ

τ_i = duration of task i in number of time intervals of size δ

Variables

$N_{i,t}$ = binary variable indicating the start of execution of task i in slot t

$R_{r,t}$ = excess amount of resource r at the start of slot t

$\Pi_{r,t}$ = amount of power or energy resource r purchased during time slot t (MW or MWh)

References

(1) Merkert, L.; Harjunkoski, I.; Isaksson, A.; Saynevirta, S.; Saarela, A., Sand, G. Scheduling and energy - Industrial challenges and opportunities. *Computers and Chemical Engineering* **2015**, 72, 183-198.

(2) Zhang, Q.; Grossmann, I. E.. Enterprise-wide optimization for industrial demand side management: Fundamentals, advances, and perspectives. *Chemical Engineering Research and Design* **2016**, 116, 114-131.

(3) Mitra, S.; Grossmann, I.E.; Pinto, J.M.; Arora, N. Optimal Production Planning under Time-Sensitive Electricity Prices for Continuous Power-Intensive Processes. *Computers and Chemical Engineering* **2012**, 38, 171-184.

(4) Zhang Q.; Cremer, J.L.; Grossmann, I.E.; Sundaramoorthy, A.; Pinto, J.M. Risk-based integrated production scheduling and energy procurement for continuous power-intensive processes. *Computers and Chemical Engineering* **2016**, 86, 90-105.

(5) Basan, N.P.; Grossmann, I.E.; Gopalakrishnan, A.; Lotero I.; Mendez, C.A. A novel MILP Scheduling Model for Power-Intensive Processes under Time-Sensitive Electricity Prices. *Ind. Eng. Chem. Res.* **2018**, 57 (5), 1581-1592.

(6) Tsay, C.; Baldea, M.; Shi, J.; Kumar, A.; Flores-Cerillo, J. Data-Driven Models and Algorithms for Demand Response Scheduling of Air Separation Units. *Computer Aided Chemical Engineering* **2018**, 44, 1273-1278.

(7) Castro, P.M.; Harjunkoski, I.; Grossmann, I.E. New Continuous-Time Scheduling Formulation for Continuous Plants under Variable Electricity Cost. *Ind. Eng. Chem. Res.* **2009**, 48, 6701-6712.

(8) Castro, P.M.; Harjunkoski, I.; Grossmann, I.E. Optimal Scheduling of Continuous Plants with Energy Constraints. *Computers and Chemical Engineering* **2011**, 35, 372-387.

(9) Zhang, X.; Hug, G.; Zico Kolter, J.; Harjunkoski, I. Demand Response of Ancillary Service from Industrial Loads Coordinated with Energy Storage. *IEEE Transactions on Power Systems* **2017**, 33 (1), 951-961.

(10) Mitra, S.; Sun, L.; Grossmann, I.E. Optimal Scheduling of Industrial Combined Heat and Power Plants under Time-Sensitive Electricity Prices. *Energy* **2013**, 54, 194-211.

(11) Merkert, L.; Castro, P.M. Optimal Scheduling of a District Heat System with a Combined Heat and Power Plant Considering Pipeline Dynamics. *Ind. Eng. Chem. Res.* **2020**, 59, 5969-5984.

(12) Hadera, H.; Ekstrom, J.; Sand, G.; Mantysaari, J.; Harjunkoski, I.; Engell, S. Integration of production scheduling and energy-cost optimization using Mean Value Cross Decomposition. *Computers and Chemical Engineering* **2019**, 129, 106436.

(13) Zhang, X.; Hug, G.; Harjunkoski, I. Cost-effective Scheduling of Steel Plants with Flexible EAFs. *IEEE Transactions on Smart Grid* **2017**, 8 (1), 239-249.

(14) Nolde, K.; Morari, M. Electrical load tracking scheduling of a steel plant. *Computers and Chemical Engineering* **2010**, 34, 1899-1903.

(15) Hadera, H.; Harjunkoski, I.; Sand, G.; Grossmann, I.E.; Engell, S. Optimization of steel production scheduling with complex time-sensitive electricity cost. *Computers and Chemical Engineering* **2015**, 76, 117-136.

(16) Pan, R.; Li, Z.; Cao, J.; Zhang, H.; Xia, X. Electrical Load Tracking Scheduling of Steel Plants under Time-of-Use Tariffs. *Computers and Industrial Engineering* **2019**, 137, 106049.

(17) Xu, W.; Tang, L.; Pistikopoulos, E.N. Modeling and Solution for Steelmaking Scheduling with Batching Decisions and Energy Constraints. *Computers and Chemical Engineering* **2018**, 116, 368-384.

(18) McCormick, G.P. Computability of Global Solutions to Factorable Nonconvex Programs: Part I- Convex Underestimating Problems. *Math. Program.* **1976**, 10, 147-175.

(19) Sundaramoorthy, A.; Maravelias, C.T. Computational Study of Network-Based Mixed-Integer Programming Approaches for Chemical Production Scheduling. *Ind. Eng. Chem. Res*. **2011**, 50, 5023-5040.

(20) Harjunkoski, I.; Maravelias, C.; Bongers, P.; Castro, P.M.; Engell, S.; Grossmann, I.E., Hooker, J.; Méndez, C.; Sand, G.; Wassick, J. Scope for Industrial Applications of Production Scheduling Models and Solution Methods. *Comput. Chem. Eng*. **2014**, 62, 161-193.

(21) Castro, P.M.; Sun, L.; Harjunkoski, I. Resource-Task Network Formulations for Industrial Demand Side Management of a Steel Plant. *Ind. Eng. Chem. Res*. **2013**, 52, 13046-13058.

(22) Pantelides, C.C. Unified Frameworks for the Optimal Process Planning and Scheduling. Proceedings of the Second Conference on Foundations of Computer Aided Operations. Cache Publications: New York, 1994.

(23) Dalle Ave G.; Harjunkoski, I.; Engel, S. A Non-Uniform Grid Approach for Scheduling Considering Electricity Load Tracking and Future Load Prediction. *Computers and Chemical Engineering* **2019**, 129(4), 106506.

(24) Castro, P.M.; Grossmann, I.E.; Veldhuizen, P.; Esplin, D. Optimal Maintenance Scheduling of a Gas Engine Power Plant using Generalized Disjunctive Programming. *AIChE J*. **2014**, 60(6), 2083-2097.

(25) Zulkafli, N.I.; Kopanos, G.M. Planning of Production and Utility Systems under Unit Performance Degradation and Alternative Resource-Constrained Cleaning Policies. *Applied Energy* **2016**, 183, 577-602.

(26) Nie, Y.; Biegler, L.T.; Wassick, J.M.; Villa, C.M. Extended Discrete-Time Resource Task Network Formulation for the Reactive Scheduling of a Mixed Batch/Continuous Process. *Ind. Eng. Chem. Res.* **2014**, 53, 17112-17213.

(27) Vieira, M.; Pinto-Varela, T.; Barbosa-Póvoa, A.P. Production and Maintenance Planning Optimisation in Biopharmaceutical Processes under Performance Decay using a Continuous-time Formulation: a Multi-objective Approach. *Computers and Chemical Engineering* **2017**, 107, 111-139.

(28) Wu, O., Dalle Ave, G., Harjunkoski, I., Imsland, L., Schneider, M., Bouaswaig, A.E.F., Roth, M. Short-term Scheduling of a Multipurpose Batch Plant Considering Degradation Effects. *Computer Aided Chemical Engineering* **2019**, 46, 1213-1218.

(29) Spuntrup, F. S.; Dalle Ave, G., Imsland, L.; Harjunkoski, I. Optimal Maintenance Scheduling for Washing of Compressors to Increase Operational Efficiency. *Computer Aided Chemical Engineering* **2019**, 46, 1321-1326.

(30) van der Klauw, T.; Hurink, J. L.; Smit, G. J. M. Scheduling of Electricity Storage for Peak Shaving with Minimal Device Wear. *Energies* **2016**, 9 (6), 465-484.

(31) Biondi, M.; Sand, G.; Harjunkoski, I. Optimization of multipurpose process plant operations; a multi-time scale maintenance and production scheduling approach. *Computers and Chemical Engineering* **2017**, 99, 325-339.

(32) Wiebe, J.; Cecílio, I.; Misener, R. Data-Driven Optimization of Processes with Degrading Equipment. *Ind. Eng. Chem. Res*. **2018**, 57, 17177-17191.

(33) Dalle Ave G.; Hernandez, J.; Harjunkoski, I.; Onofri, L.; Engell, S. Demand Side Management Scheduling Formulation for a Steel Plant Considering Electrode Degradation. *IFAC-PapersOnLine* **2019**, 52 (1), 691-696.

(34) Castro, P.M.; Harjunkoski, I.; Grossmann, I.E.. Discrete and Continuous-time Formulations for Dealing with Break Periods: Preemptive and Non-Preemptive Scheduling. *European Journal of Operational Research* **2019**, 278, 563-577.

(35) Dowling, A.W.; Kumar, R.; Zavala, V.M. A Multi-Scale Optimization Framework for Electricity Market Participation. *Applied Energy* **2017**, 190, 147-164.

(36) Lee, H.; Gupta, D.; Maravelias, C.T. Systematic Generation of Alternative Production Schedules. *AIChE J*. **2020**, https://doi.org/10.1002/aic.16926.